

Adsorption hysteresis in porous materials

Christopher G.V. Burgess, Douglas H. Everett* & Stuart Nuttall

Department of Physical Chemistry, University of Bristol, Bristol BS8 1TS, U.K.

ABSTRACT - Adsorption hysteresis exhibits a wide range of phenomena dependent on the nature of both the adsorbent and the adsorptive, and on the temperature. Some of these features are described and an outline is given of their interpretation in terms of the physical processes involved. Particular attention is paid to the changes in the size and shape of hysteresis loops brought about by changes in temperature, which are discussed in terms of 'hysteresis phase diagrams'. 'Hysteresis critical temperatures' are identified and linked to recent theories of capillary condensation.

INTRODUCTION

Adsorption hysteresis in porous materials can take on many forms, characterised both by the shapes of the hysteresis loops and by the way in which they depend on temperature. Some of these features are illustrated in Fig.1, taken from the work of Amberg, Everett, Ruiters and Smith (ref.1). Thus the adsorption of CO₂ by Vycor glass at pressures up to one atmosphere is reversible over a wide range of temperature (Fig.1A). This contrasts with the behaviour of N₂O which adsorbs reversibly at low temperatures but exhibits hysteresis at higher temperatures (Fig.1B). Conversely, when CO₂ is adsorbed by porous carbon (Fig.1C), reversible adsorption at higher temperatures gives way to an increasing degree of hysteresis as the temperature is lowered. When N₂O is adsorbed by porous carbon (Fig.1D), hysteresis is observed both at high and low temperatures, with an intermediate range in which adsorption is reversible. The difference between the behaviour of CO₂ and N₂O adsorbed by porous glass up to atmospheric pressure arises because the triple point pressure for N₂O is below atmospheric, whereas that for CO₂ is above. The experimental temperature range for N₂O thus includes the triple point temperature, while for CO₂ this temperature was not reached. By working at higher temperatures and pressures up to and beyond the triple point of CO₂, hysteresis should also be observed for the CO₂/Vycor system. The work of Burgess, Fig.2 (ref.2), confirmed this. Similar behaviour in the case of the CO₂/silica gel system was demonstrated by Dubinin and his coworkers (ref.3). Burgess's work was extended by Nuttall (ref.4) who studied the adsorption of Xe on both porous glass and activated carbon (Figs.3 & 4). An important feature of these systems is the way in which the hysteresis loops develop somewhat below the triple point temperature of the adsorptive, shrink as the temperature is raised and disappear some distance below the bulk critical temperature. However, there are marked differences between the behaviour of porous glass and active carbon. Thus with both CO₂ and Xe on porous glass, the shrinkage of the hysteresis loop involves a decrease in both the height and width of the loop, while for Xe on active carbon the main change is in the width of the loop, the height varying relatively slowly. The difference between the two substrates is brought out more clearly if the data are plotted as a function of pressure rather than its logarithm (Figs.5.a & b). The loop in the case of porous glass has steep sections and closes below p^* (type H1 in the IUPAC classification, ref.5), while for porous carbon the loop is elongated along the pressure axis and closes only at the saturation vapour pressure. (type H4).

As pointed out by de Boer long ago (ref.6) these differences are to be attributed to different pore structures. The former case is associated with corpuscular porous bodies, while the latter is indicative of slit-shaped pores. To illustrate this Rohas (ref.7, Fig.6) prepared mesoporous carbons consisting of packed non-microporous spheres, whose structure can be ascertained by scanning electron microscopy. The benzene isotherms for these materials exhibit steep vertical sections, closely similar to those predicted by Kiselev and Karnaukhov (ref.8) for packed spheres.

Mention should also be made of the phenomenon of low pressure hysteresis in which the desorption curve falls rapidly at some characteristic pressure, but fails to meet the adsorption branch and runs more or less parallel to it to very low pressures (ref.9). This 'low pressure hysteresis' is often found when the size of the adsorptive molecule is commensurate with the average pore size of the adsorbent.

INTERPRETATIONS OF ADSORPTION HYSTERESIS

Different types of adsorption hysteresis arise from different physical mechanisms. Thus the low temperature hysteresis found well below the triple point in the case of CO_2 and N_2O adsorbed by active carbon has been attributed (ref.1) to the epitaxial growth of solid-like adsorbate whose structure is governed initially by that of the substrate. When the adsorbed layer thickens a limit is reached at which the structure switches irreversibly to that of the crystal lattice of the bulk CO_2 or N_2O . The hysteresis can thus be related to hysteresis in a solid transition brought about by changing the amount adsorbed.

Low pressure hysteresis is thought to arise from swelling of the adsorbent. In many cases the deformed structure does not relax even when the adsorbate has been removed by outgassing at a high temperature, and the original adsorbent properties are only recovered after a long period of annealing. One piece of evidence for this

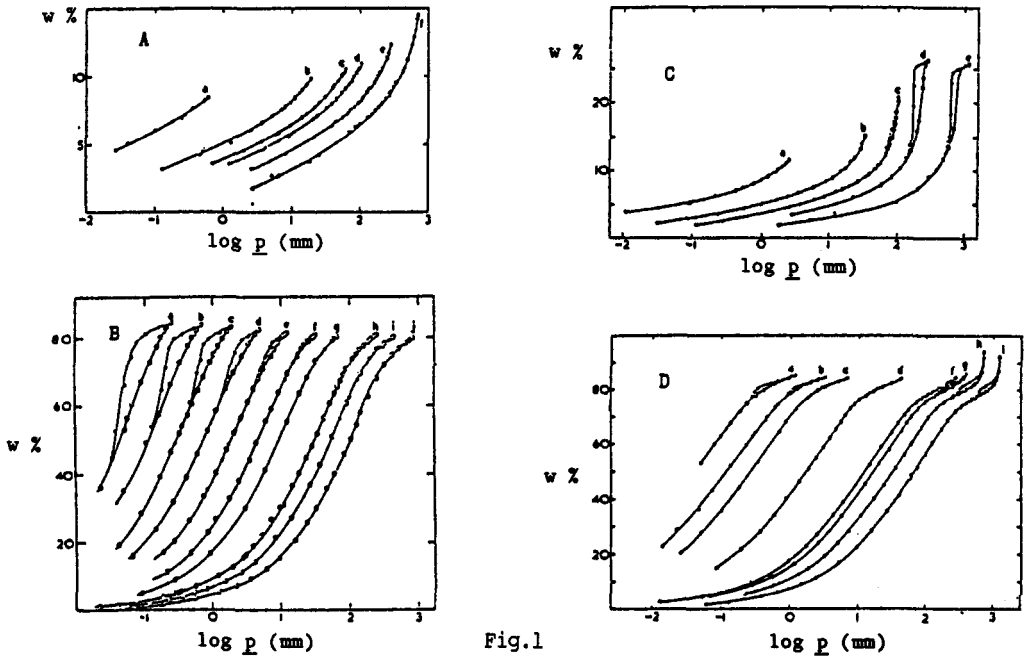


Fig.1

- A. Adsorption of CO_2 by Vycor from 135.2K(a) to 193.2K(f)
 B. Adsorption of CO_2 by active carbon from 130.4K(a) to 196.3K(j)
 C. Adsorption of N_2O by Vycor from 132.5K(a) to 193.0K(e)
 D. Adsorption of N_2O by active carbon from 130.3K(a) to 192.8K(i) Plotted as weight % against $\log(p/\text{mmHg})$

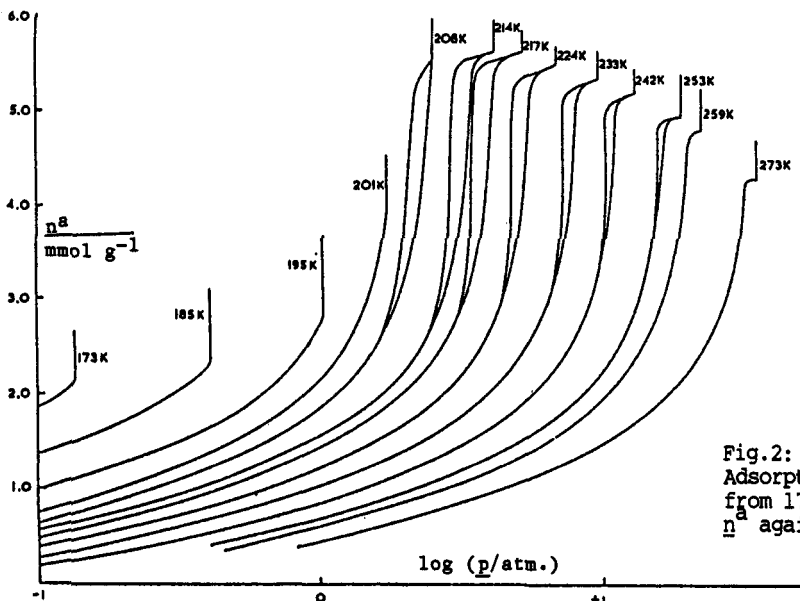


Fig.2:
 Adsorption of CO_2 by porous glass from 173K to 273K, plotted as n^a against $\log(p/\text{atm.})$

explanation is that whereas a given porous carbon may show a hysteresis loop which closes normally when adsorbing a flat molecule such as benzene, low pressure hysteresis occurs when the adsorptive molecule is of similar molar volume, but of roughly spherical shape, such as 2,2-dimethyl butane. Moreover, there seems to be a critical pressure which, if exceeded in the adsorption step, leads to low pressure hysteresis. This suggests that the swelling pressure must exceed the yield stress of the pore system. Furthermore, the low pressure hysteresis for a given adsorptive can be eliminated by increasing the pore size by activation. This phenomenon is clearly related to the swelling and hysteresis in the adsorption of vapours by clays, the thermodynamics of which is dealt with by Barrer in his contribution to this Symposium (ref.10).

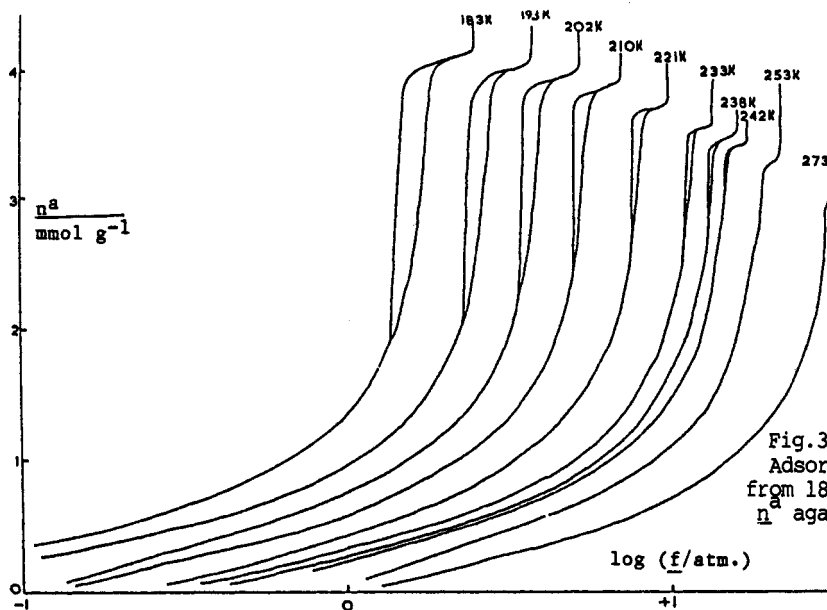


Fig.3: Adsorption of Xe by porous glass from 183K to 273K plotted as n^a against $\log(f/\text{atm.})$

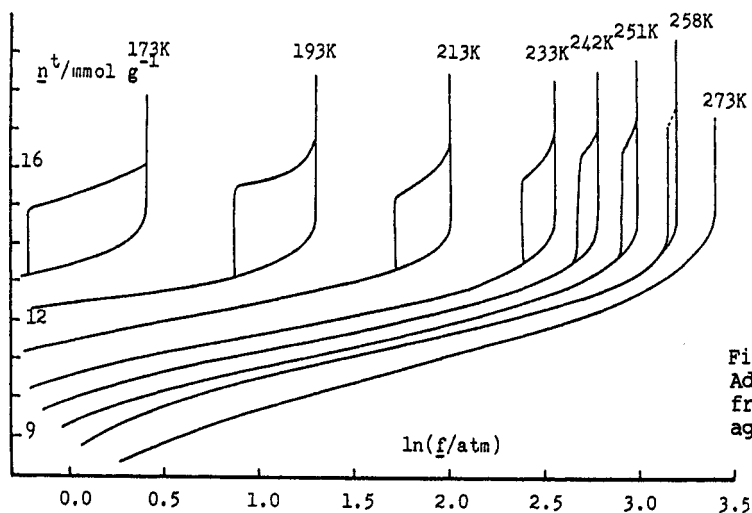


Fig.4: Adsorption of Xe by active carbon from 173K to 273K plotted as n^t against $\ln(f/\text{atm.})$

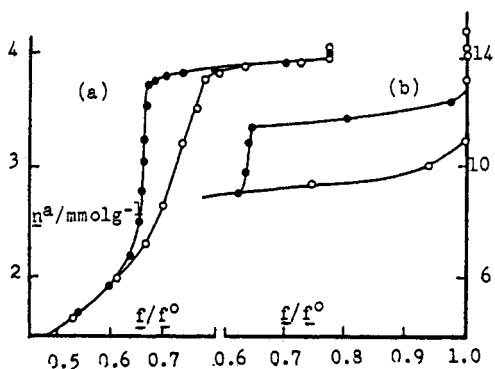


Fig.5: Comparison of adsorption of Xe by porous glass (a) and active carbon (b) plotted as n^a against f/f^0 .

CAPILLARY CONDENSATION HYSTERESIS

Hysteresis at temperatures near to and above the triple point of the bulk adsorptive is attributed to capillary condensation, and has attracted the attention of colloid and surface scientists for many decades. It has recently become a topic of active consideration by several groups of theoretical physicists, using modern statistical mechanical and computational techniques.

The origin of capillary condensation in terms of surface forces has been studied extensively by Deryagin and Churaev (ref.11). Everett and Haynes (ref.12) examined the mechanism of condensation in cylindrical capillaries using bulk thermodynamic concepts: some of their main conclusions have been confirmed by very recent computer simulation studies (ref.13). Capillary condensation in packed spheres has been studied in detail by Kiselev and Karnaukhov (ref.8) and by Wade (ref.14).

Of crucial importance is the question as to what determines the limits of capillary condensation. The transition from adsorption to condensation is clearly dependent on the balance between the interactions of the adsorbed molecules with the solid surface and with themselves. When the adsorbed layer achieves some critical thickness, the the outer surface, farthest from the solid substrate, adopts a liquid-like structure and exhibits a surface tension. When this stage is reached capillary condensation, controlled by surface forces in the liquid occurs, even though near the three phase contact line the shape of the meniscus may be dominated by surface forces emanating from the solid (ref.15). Pore size and pore shape must also play a part. If the pores are too small, then all the adsorbed molecules remain under the influence of the surface forces, and there are too few adsorbed molecules for the intermolecular forces between them to lead to condensation. Similarly, an increase in temperature will decrease the tendency for condensation. Thus one may anticipate the existence of a critical thickness of the adsorbed layer, a lower limit to pore size and an upper limit of temperature beyond which capillary condensation is absent.

The work of Burgess and Nuttall provides quantitative information on these factors. Evidence that condensation can occur in a given structure only when the adsorption exceeds a certain limit comes from an analysis of the lower, reversible sections of the isotherms, using the extended BET-equation first suggested explicitly by Anderson (ref.16). As pointed out by Guggenheim, however, (ref.17), this equation is implicit in Langmuir's Case VI (ref.18). The statistical basis for this equation has been clarified by Guggenheim and by Hill (ref.19). In effect the saturation vapour pressure, p^0 , of the adsorptive in the BET-equation is replaced by an adjustable parameter p^* whose value is chosen to give the best representation of the experimental isotherm: p^* is only equal to p^0 when the molecules in the multilayer have liquid-like properties. In the case of adsorption at high pressures, the pressure must, of course, be replaced by the vapour fugacity. The extended equation is found to have wide applicability (ref.20). It gives an excellent representation of the adsorption of CO_2 and N_2O by porous glass over the temperature range 173-273K, and up to a critical adsorption at which substantial deviations occur.

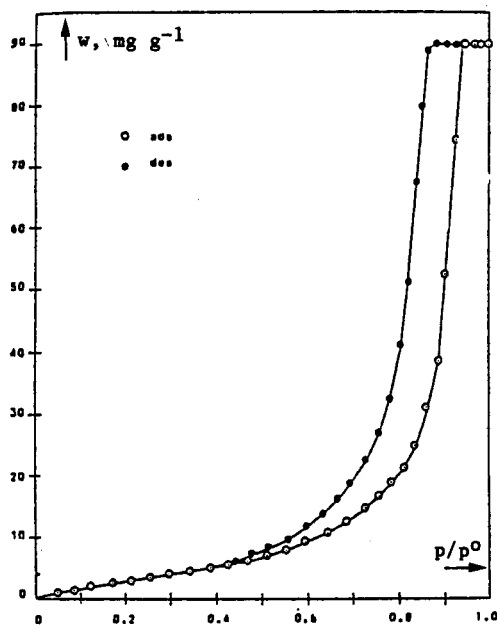


Fig.6:
Adsorption of benzene by mesoporous 'spherical' carbon at 25°C, plotted as weight adsorbed against relative pressure p/p^0 .

These deviations may be attributed to the onset of capillary condensation, and occur, approximately, at the lower limit of the hysteresis loop. The amount adsorbed at this point is very roughly twice the 'monolayer capacity'. The correlation is not exact but suggests that for condensation to occur a minimum of two molecular layers must be formed on the surface.

The dependence of the position of the lower limit of the hysteresis loop on pore size and temperature presents a fundamental problem. In the past it has been interpreted by considering desorption from pores of steadily decreasing dimensions (ref.21). Thus as menisci retreat into smaller and smaller pores, the pressure difference across the vapour/liquid interface increases. The pressure within the liquid falls and eventually changes sign, when the liquid is subjected to a tension. So long as this tension is less than the ultimate tensile strength of the liquid the meniscus is stable. If it is exceeded the liquid state becomes unstable and it is no longer possible for a two-phase system to exist in the pores. This is an attractive explanation and has been supported by a certain amount of experimental evidence. Dubinin and Kadlec (ref.22) related this explanation to the intermolecular forces in the liquid, while Burgess and Everett (ref.23) compared the ultimate tensile strengths calculated from experimental data with those corresponding to various equations of state of the liquid. Despite this evidence we now believe that this interpretation is unacceptable as a general explanation.

The problem has been attacked recently by applying statistical mechanical arguments to the case of molecules confined in a space whose dimensions are not too different from the size of the adsorbed molecule. In effect, one studies the influence of confinement on the liquid-vapour phase diagram. Using mean field and density gradient methods, which were originally developed to model the molecular state of the bulk liquid/vapour interface, Evans and his co-workers at Bristol (ref.24), and Gubbins and his co-workers at Cornell (ref.25), among others (ref.26), have shown that 'capillary condensation' should disappear both when the pore dimensions decrease at constant temperature, and when, for a given pore size, the temperature is increased. It turns out, for example, that for slit-like pores of width H , $(1/H)$ and T play the same role in the theoretical equations: capillary condensation disappears when either $(1/H)$ or T exceed certain critical values. The tensile strength of the liquid does not appear as a factor in these theories.

THE HYSTERESIS PHASE DIAGRAM

It is instructive to examine our experimental data in the light of the recent theoretical developments. Thus the locus of the extremes of the hysteresis loops (which delineates the region of co-existence of vapour and condensed liquid) defines a 'hysteresis phase diagram'. This may be expressed in terms of alternative pairs of variables. Fig.7 shows, for the CO_2/Vycor system, the phase diagram expressed in terms of the total amount adsorbed, n , and the temperature. Here n_{t} is calculated from the Gibbs surface excess \bar{n} by assuming a value of $0.214 \text{ cm}^3 \text{ g}^{-1}$ for the pore volume of Vycor, a value consistent with the volume estimated from the Gurvich rule applied to the adsorption of benzene and other organic liquids. This diagram resembles closely that for a bulk liquid, although the region below the triple point deserves special mention. In the case of CO_2/Vycor the dotted portion of this curve is somewhat speculative. At 193K the adsorption is reversible (Fig.1A) so that the phase diagram must close somewhere between 193 and 207K. At lower temperatures the maximum adsorption at the saturated vapour pressure varies rapidly (triangles in Fig.7), and it is presumed that the minimum in the phase diagram lies on the extrapolation of this curve. This presumption is supported by the data for $\text{N}_2\text{O}/\text{Vycor}$ (Fig.1C), where the shrinkage of the loop towards a lower temperature limit is observed experimentally (Fig.8). We note that in both cases hysteresis persists well below the bulk triple point in accordance with the thermodynamic expectation that the triple point of liquid condensed in narrow pores is depressed. A decrease in the width of a hysteresis loop as the temperature is lowered has also been observed by Hien and Serpinski (ref.27) in the case of the adsorption of pentane by silica gel. However, in their case this narrowing occurs far above the triple point of pentane.

At the upper hysteresis critical temperature, $T_{\text{c}}(h)$, the distinction between liquid and vapour in the pore space disappears and the surface tension between them tends to zero. In this region the pressure difference across the meniscus must also tend to zero: an interpretation based on the build-up of a negative pressure in the liquid phase must be invalid, at least at temperatures approaching $T_{\text{c}}(h)$.

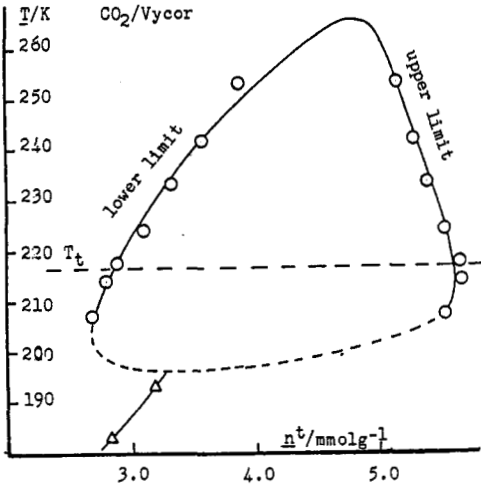


Fig. 7: Hysteresis phase diagram of CO₂ adsorbed by Vycor, plotted as \bar{T} against n^t at the upper and lower closure points of the hysteresis loops

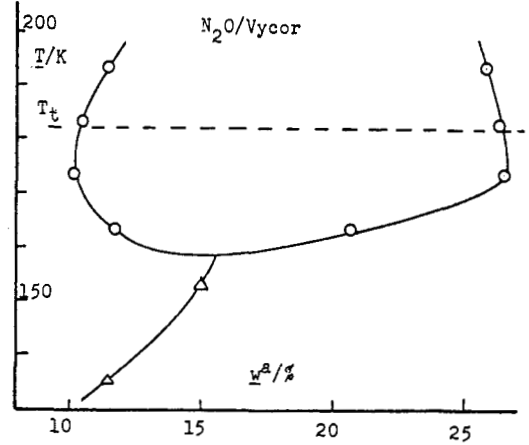


Fig. 8: Hysteresis phase diagram of N₂O adsorbed by Vycor showing evidence for closure of the hysteresis diagram at low temperatures

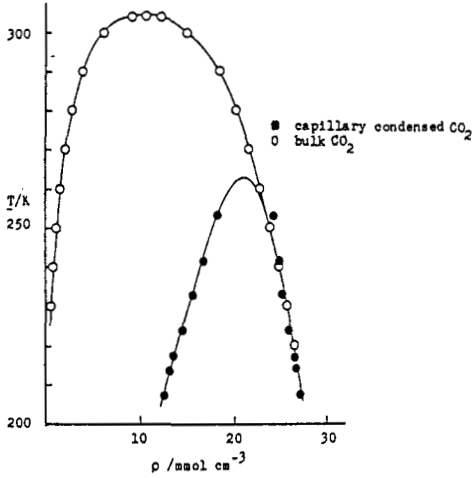


Fig. 9: Comparison of hysteresis phase diagram for CO₂/Vycor with phase diagram of bulk CO₂

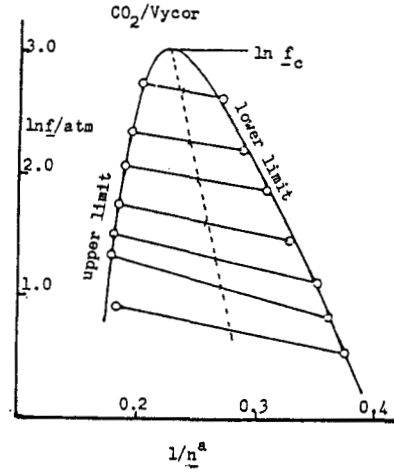


Fig. 10: Hysteresis phase diagram for CO₂/Vycor in $\ln f_c$ against $1/n^a$ co-ordinates

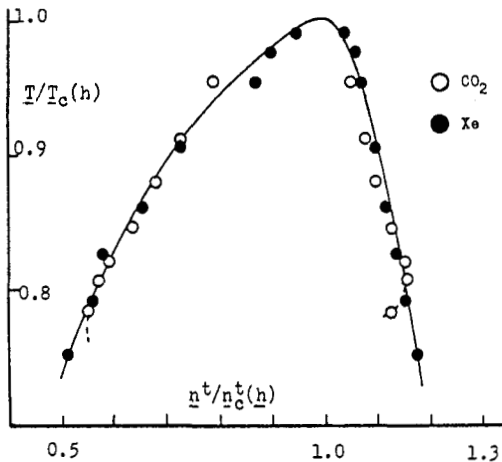


Fig. 11: Comparison of hysteresis phase diagrams for CO₂/Vycor and Xe/Vycor in reduced units

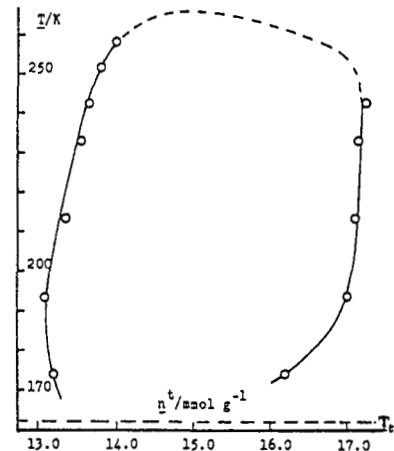


Fig. 12: Hysteresis phase diagram for Xe/active carbon

Comparison with the bulk phase diagram is made more explicit if n^t is replaced by ρ , the density of adsorbed material at the upper and lower limits of the hysteresis loop. Fig.9 shows that in a porous medium the phase diagram of the bulk system is both lowered and narrowed. Another representation is to plot $\ln f$ against $1/n^t$ which enables the fugacity at the critical temperature to be determined (Fig.10). Comparison between the CO_2 and Xe systems may be made by expressing their phase diagrams in terms of the reduced quantities $T/T_C(h)$ and $n/n_C(h)$, where $n_C(h)$ is the value of n^t at the hysteresis critical point (Fig.11). The points for the two systems lie on a common curve.

A preliminary comparison may be made with the theoretical predictions of Evans *et al.* According to the simplest form of their theory the capillary condensation critical temperature— which we have called the hysteresis critical temperature— is determined for cylindrical pores of radius R_C by the approximate relationship

$$\frac{T_C - T_C(h)}{T_C} \sim \frac{\lambda}{R_C} \quad (1)$$

where T_C is the bulk critical temperature. λ may be taken as equal to \underline{d} the molecular diameter, and the proportionality factor assumed to be unity. Then with $\underline{d} = 0.41\text{nm}$ for both Xe and CO_2 (ref.28) we obtain $R_C = 2.59 \pm 0.05$ or 3.18 ± 0.40 nm respectively. The agreement between the results for Xe and CO_2 is reasonable bearing in mind that it is a crude approximation to take CO_2 as a spherical molecule, while in this case it is difficult to establish $T_C(h)$ with great precision. The median Kelvin radii calculated from the Xe isotherms at lower temperatures are 2.4nm for the adsorption branch and 1.8nm for the desorption branch. Correction for film thickness raises these to 3.4 and 2.8nm respectively. The broad agreement between the various estimates of pore size suggests that in this case at least relation (1) can, to a first approximation, be taken as an equality.

The Xe/active carbon system exhibits a rather different type of behaviour. The initial adsorption occurs reversibly in micropores, and the adsorption isotherm is generally Langmuirian in shape. In fact this part of the isotherm can also be represented with high accuracy by the extended BET-equation, but now with a relatively high value of f^*/f_0 , typically 6-8 depending on the temperature. We recall that the extended equation leads to the Langmuir equation when $f^*/f_0 \rightarrow \infty$. Hysteresis in this system is therefore associated with capillary condensation in mesopores consisting of the interstices between microporous sub-structures. The data suggest that this does not occur until the vapour approaches the bulk saturation pressure. The reasons for this can only be the subject of speculation at the moment. It may be that the mesopores are essentially slit-like, in which condensation is delayed. Alternatively it may be controlled by the meniscus configurations at the mouths of micropores where they open on to the surface of the substructures. The hysteresis phase diagram in this case differs markedly from those for adsorption in porous glass (Fig.12), since the two branches in the T, n^t diagram remain widely separated until close to the hysteresis critical temperature: the decrease in size of the hysteresis loop occurs mainly through a decrease in its width. Extrapolation of a graph of the width $\Delta(\ln f)$ against $1/T$ indicates a critical temperature of 265K, or $T_C(h)/T_C$ of 0.915, substantially higher than that found for the Xe/Vycor system (0.842). The top of the phase diagram, shown dotted, must be very flat, in contrast to that for the Vycor systems. Again there is evidence for a contraction of the phase diagram at lower temperatures near the triple point.

It is interesting to speculate whether these differences could arise from the different dimensionalities of the pore structures. In Vycor the pores have a three dimensional character (a model of cylindrical capillaries can only be a rough approximation), while those in porous carbon are thought to be slit-like in character. The shape of the phase boundary near a critical point is known, theoretically, to depend on the dimensionality of the system. The curves for two-dimensional systems are flatter (with a critical exponent $\beta = 1/8$) than those for a three-dimensional system ($\beta = 1/3$) (ref.29). Because of the difficulty of establishing the exact form of the hysteresis phase diagram near the critical point it is neither possible to test this hypothesis quantitatively, nor at this stage to use the data to deduce the dimensionality of the pore systems concerned.

The way in which the hysteresis phase diagram arises can be illustrated in the case of a single pore in terms of a van der Waals-type equation of state of material in a pore, and its variation with temperature (Fig.13). Hysteresis then results from the persistence of metastable states in one or both of the evaporation or condensation processes. As the temperature is raised the loop shrinks in size and at the critical temperature it degenerates into a point of inflexion. One thus obtains a three dimensional curve, which is essentially a spinodal curve, whose projections on the (T, v) or (T, f) planes correspond to the experimental curves.

This type of behaviour is predicted on the basis of several theories. For example the width of the loop (in $\ln p$ vs n co-ordinates) should according to the model of Everett and Haynes (ref.12) be proportional to σv (where σ is the surface tension and v the molar volume); while both Evans *et al.* (ref.25) and Gubbins *et al.* (ref.26) predict similar behaviour. We comment that in the latter theories mechanical instability on evaporation occurs at the minimum in the van der Waals loop, which does not necessarily extend into the negative pressure region. The situation is of course more complicated in real systems because of the distribution of pore sizes.

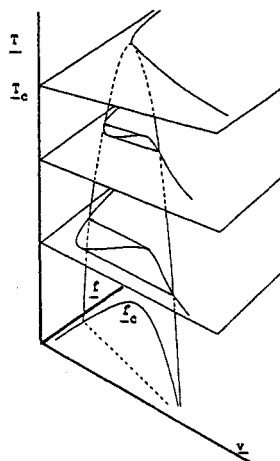


Fig.13:
Interpretation of the hysteresis phase diagram in terms of the variation of the state with temperature

OTHER FACTORS

In this paper several important factors affecting the detailed behaviour of systems showing adsorption hysteresis have been neglected. The most important of these are the effects of pore size distribution and network or percolation phenomena. Although these will undoubtedly influence many details of the phenomena discussed above, in particular the shape of desorption curves, the broad conclusions concerning the nature of capillary condensation processes should still be valid.

REFERENCES

1. C.H.Amberg, D.H.Everett, L.H.Ruiter & F.W.Smith, in 'Surface Activity', J.H.Schulman (Ed.), Butterworths, London, 1957, vol.2, p.2.
2. C.V.G.Burgess, Ph.D.Thesis, Bristol, 1971.
3. M.M.Dubin, B.P.Bering, V.V.Serpinskii & B.N.Vasilev, in 'Surface Phenomena in Chemistry and Biology', J.F.Danielli, R.G.A.Pankhurst & A.C.Riddiford (Eds.) Pergamon Press, London, 1958, p.172.
4. S.Nuttall, Ph.D.Thesis, Bristol, 1974.
5. K.S.W.Sing, *et al.*, Reporting Physisorption Data for Gas/Solid Systems, *Pure & Appl. Chem.*, **57**, 603 (1985).
6. J.H.de Boer, in 'The Structure and Properties of Porous Materials' (Colston Papers, vol.X), D.H.Everett & F.S.Stone (Eds.), Butterworth, London, 1958, p.68.
7. F.Rojas, Ph.D.Thesis, Bristol, 1982; D.H.Everett & F.Rojas, *J.Chem.Soc., Faraday Trans.1*, **84**, 1455 (1988).
8. A.P.Karnaukhov & A.V.Kiselev, *Zhur.fiz.Khim.*, **34**, 2146 (1960); A.P.Karnaukhov, *Kinetika i Kataliz*, **12**, 1025, 1235 (1971).
9. A.Bailey, D.A.Cadenhead, D.H.Davies, D.H.Everett & A.J.Miles, *Trans.Faraday Soc.*, **67**, 231, (1971).
10. R.M.Barrer, This Symposium.
11. B.V.Deryagin & N.V.Churaev, *J.Colloid Interface Sci.*, **54**, 157 (1976).
12. D.H.Everett & J.M.Haynes, *J.Colloid Interface Sci.*, **38**, 125 (1972); D.H.Everett, *J.Colloid Interface Sci.*, **52**, 189, (1975).
13. G.S.Heffelfinger, F.van Swol & K.E.Gubbins, *J.Chem.Phys.*, **89**, 5202, (1988).
14. W.H.Wade, *J.Phys.Chem.*, **68**, 1029 (1964); **69**, 322 (1965).
15. B.V.Deryagin, *Acta phys.chim.,URSS*, **12**, 181, (1940); in 'Surface Activity', J.H.Schulman (Ed.), Butterworths, London, 1957, vol.2, p.153.
16. R.B.Anderson, *J.Amer.Chem.Soc.*, **68**, 686 (1946); cf. S.Brunauer, J.Skalny & E.E.Bodor, *J.Colloid Interface Sci.*, **30**, 546 (1969).
17. E.A.Guggenheim, 'Applications of Statistical Mechanics', Clarendon Press, Oxford, 1966, Chap.11.
18. I.Langmuir, *J.Amer.Chem.Soc.*, **40**, 1375, (1918).
19. T.L.Hill, 'Statistical Mechanics', McGraw-Hill, New York, 1956, Appendix 5.
20. C.V.G.Burgess, D.H.Everett, D.Llewellyn & S.Nuttall, in preparation; D.H.Everett, *Proc. 5th.Hungarian Internat.Conf.on Colloids*, 1988, to appear.
21. R.K.Schofield, *Discuss.Faraday Soc.*, **3**, 105, (1948); E.A.Flood, in 'The Solid-Gas Interface', E.A.Flood (Ed.), Dekker, New York, vol.1, Chap.1; D.H.Everett, *idem*, vol.2, Chap.36.
22. O.Kadlec & M.M.Dubin, *J.Colloid Interface Sci.*, **31**, 479 (1969).
23. C.G.V.Burgess & D.H.Everett, *J.Colloid Interface Sci.*, **33**, 611 (1970).
24. R.Evans, M.B.Marconi & P.Tarazona, *J.Chem.Soc. Faraday Trans.2*, **82**, 1569, (1986); *J.Chem.Phys.*, **84**, 2376, (1986); P.C.Ball & R.Evans, paper submitted to *Langmuir*, 1988.
25. B.K.Peterson, J.R.B.Walton & K.E.Gubbins, *J.Chem.Soc. Faraday Trans.2*, **82**, 1789, 1986.
26. e.g. D.Nicholson, *J.Chem.Soc. Faraday Trans.1*, **71**, 239 (1975).
27. N.T.M.Hien & V.V.Serpinskii, *Izvest. Akad. Nauk SSSR, Ser.Khim.*, **11**, 2421 (1987).
28. J.O.Hirschfelder, C.F.Curtiss & R.B.Bird, 'Molecular Theory of Gases and Vapours', Wiley, New York; Chapman & Hall, London, 1954, Appendix, Table IA.
29. H.E.Stanley, 'Phase Transitions and Critical Phenomena', Clarendon Press, Oxford, 1971, pp. 10,47.